
# Chapter 3
# Classification of Footprint Models

Footprint models constitute quality-assurance tools that can be used to support the interpretation of scalar, flux, and concentration measurements. The purpose of the present chapter is to provide the reader with an overview of key developments in footprint modeling. This chapter also highlights the key features and limitations inherent to each model. Here, the authors seek to provide sufficient information to empower the reader to select the most appropriate model for the purpose at hand. The reader is thus strongly encouraged to read the original papers for a more exhaustive and thorough description of these models.

In a nutshell, five approaches are presently available to calculate the flux footprint to the experimentalists and modelers alike: (1) Numerous forms of analytical solutions with varying degrees of complexity, whether 1D, 2D or even with the full 3D formulation, (2) Lagrangian simulations based on stochastic modeling of inhomogeneous turbulence, (3) Higher-order closure models, (4) Finally, in the hierarchy of footprint models, Large-Eddy Simulation, and (5) A combination of the above methods. Each category will be reviewed briefly. Table 1.3 presents some of the most important footprint models.

In the selection of a footprint model, the experimentalist is advised to consider several important criteria: (1) Complexity of the site as defined by roughness characteristics, vegetation types and biological, chemical and physical characteristics encompassed within the footprint area, topography, (2) Extent and depth of the experimental database for the site in question, (3) Range of atmospheric stabilities covered by the flux measurement campaign, (4) Purpose of application of the footprint model to determine the degree of accuracy needed in deriving credible footprint estimates, and (5) Level of familiarity and ease of use of each

M. Y. Leclerc and T. Foken, *Footprints in Micrometeorology and Ecology*,
DOI: 10.1007/978-3-642-54545-0_3, © Springer-Verlag Berlin Heidelberg 2014

footprint model, along with a working knowledge and understanding of the underlying hypotheses and assumptions.

Stationarity assumption aside ($d/dt = 0$ over the period of time), most models here represent adequately the state of the atmosphere. The turbulent transport of a scalar during the day over flat terrain is also generally well represented while rapid progress is being made to incorporate forcings such as that induced by the presence of hydrostatic pressure gradient arising from sloping terrain and discontinuities in roughness characteristics of the terrain over the area encompassed by an atmospheric exchange measurement. Moreover, recent progress is also being made quantifying and interpreting, not over a 2D "surface", but over a 3D surface complete with a vertical distribution of sources and sinks in addition to that of the horizontal distribution of the same sources. This is a great step forward in the analysis of surface-atmosphere exchange over tall forest canopies. The following overview ranges from the simplest, most field-ready footprint models such as the analytical solutions to the sophisticated CPU-intensive Large-Eddy Simulation.

## 3.1 Analytical Footprint Models

Analytical flux footprint models based either on exact or approximate solutions to the advection-diffusion equation aim at providing the first description for the vertical diffusion of material released at the surface. The majority of the models described here assumes an infinite crosswind line source of passive scalars and often resort to the use of power laws of height-dependent wind speed and eddy diffusivity. Some of the historical developments, concepts, and equations were described earlier in Chap. 2.

The analytical approach to footprint modeling is attractive in that the calculations are relatively few, easy, and quick to perform. However, analytical solutions to the advection-diffusion equation, despite their level of refinement, still have a limited ability to reproduce the diffusion process correctly is limited in many cases. Present analytical solutions for ground-level releases generally require a smooth surface, precluding their use immediately above orchards or forest canopies. The vast majority of these solutions ignore both the effect of atmospheric stability on the flow field and the height-dependence of eddy diffusivity. A notable exception is the work of Horst and Slinn (1984) whose predictions (precursors to its reformulation in terms of flux footprint functions by Horst and Weil 1992) compare well with experimental results in near-neutral conditions. However, the discrepancy between their solution and experiments increases as stability departs from neutral conditions. While powerful, its use is also not straight forward and requires the inclusion of ill-defined constants. These analytical solutions assume that the streamwise diffusion is negligible when compared with the advective component of the flow. This fact should be kept in mind for calm conditions. None of these footprint models work very well in the roughness sub-layer, inside canopies, for conditions of free convection and moderately stable conditions, and outside the atmospheric surface layer. They are thus expected to provide the highest degree of realism for cases where the mean flow is much larger than the turbulence intensity, i.e. $\overline{u(z)} \gg u'$ with $\overline{u(z)}$ for mean horizontal wind velocity in the height $z$ und $u'$ for its turbulent fluctuations.

### *3.1.1 The Schuepp et al. (1990) Approach*

With the intent of incorporating a footprint analysis as part of a flux analysis package, Schuepp et al. (1990) formulated a simple approximate one-dimensional analytical solution to the diffusion equation proposed by Gash (1986) in terms of ***footprint***. That approximate solution is based on Calder's (1952) early work. At that time, Schuepp et al. (1990) ignored the van Ulden (1978) approach. For comparison, Schuepp et al. (1990) proposed an approach with a shape parameter $r = 1$ (and $A = B = 1$, see Sect. 2.4.1). A brief review is presented here.

If one considers an infinite crosswind area source of uniform flux density which satisfies the flux boundary condition of 0 for $x \leq 0$ (outside the source area) and $Q_0$ for $x > 0$, the concentration $\chi(x, z)$ at horizontal distance $x$ and height $z$ distribution is given by

$$\chi(x,z) = -\frac{Q_0}{\kappa u_* x} exp^{-\frac{uz}{\kappa u_* x}}, \tag{3.1}$$

compare with the more general Eq. (2.82). The flux distribution can be calculated with Eq. (2.3) using the turbulent diffusion coefficient Eq. (2.7) and the concentration gradient by differentiating Eq. (3.1) with respect to $z$

$$\frac{\partial \chi(x,z)}{\partial z} = -\frac{Q_0}{\kappa u_* x} exp^{-\frac{uz}{\kappa u_* x}}\Big|_0^x. \tag{3.2}$$

The total sum of the contributions from all elements of the upwind surface flux with the footprint is the spatial weighted elemental emission

$$Q_\chi(z) = \sum_{i=1}^{n} Q_i exp^{-\frac{uz}{\kappa u_* x}}\Big|_{x_{i-1}}^{x_i}. \tag{3.3}$$

Equation (3.3) thus defines the one-dimensional "footprint". The relative contribution to the vertical flux $(\frac{1}{Q_0}\frac{dQ}{dx})$ from $x = 0$ to infinity can be used to determine the position of the peak of the footprint ($x_{\max}$), i.e. the area to which the observation at is most sensitive is,

$$x_{\max} = \frac{u}{u_*}\frac{(z-d)}{2\kappa}. \tag{3.4}$$

The above solution, however compact and simplified, does not include the influence of atmospheric stability on the behavior of the spatial extension of the footprint; in addition, this solution is limited to applications over smooth terrain.

### 3.1.2 The Schmid and Oke (1990) approach

Building upon the work of Pasquill (1972), Schmid and Oke (1990) developed a ***reverse plume source-area model*** (SAM) in a study focusing mostly on the identification of the maximum effect source location to a reference location on the basis of Fick's diffusion law for scalars (Eq. 2.76). Using the probability density function (pdf) plume of Gryning et al. (1987), Schmid and Oke (1990) derived an equation to establish an a priori selected most important source areas $\omega$ to a concentration measurement at a point, and to describe the influence of that particular source area to a reference (e.g. sensor) location. The identification of the sensitive regions to a concentration measurement is given with the function

$$P = \iint_{\omega=\omega_P} Q(x,y)dxdy \Big/ \int_{-\infty}^{\infty}\int_{0}^{\infty} Q(x,y)\,dx\,dy \tag{3.5}$$

with $P$ being the portion of the total integrated effect controlled by a $P$-criterion source area bounded by the weight distribution function isopleths $\omega = \omega_P$, Schmid and Oke (1990) determined the concentration distribution from a continuous point source of a passive scalar. The schema of this reverse plume source-area model is illustrated in Fig. 3.1.

The Schmid and Oke (1990) study incorporates the influence of non-neutral atmospheric stability on resulting ***concentration footprints***. The approach of that study is based on the use of self-similar profiles of wind velocity and eddy diffusivity expressed by power laws matched to Monin-Obukhov similarity surface-layer profiles (Gryning et al. 1987).

### 3.1.3 The Family of Horst and Weil's (1992) Analytical Solution

This 'family' includes analytical solutions to the advection-diffusion equation originating from Horst and Weil (1992) with subsequent improvements (Horst and Weil 1994, 1995; Schmid 1994; Finn et al. 1996; Schmid 1997; Haenel and Grünhage 1999; Horst 1999). A leapfrog step was made subsequently by Kormann

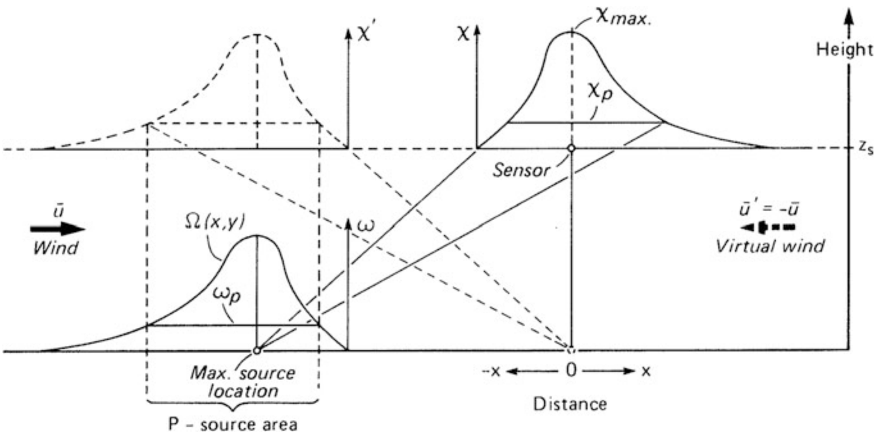


**Fig. 3.1** Schematic cross-section of a *P*-criterion source area according to Schmid and Oke (1990): the source weight distribution $\omega$ is equivalent to the plane projection of the effect-level projection, at a height $z_m$ of the virtual source beneath the sensor (and with a virtual wind in the reverse direction), Published with kind permission of © Royal Meteorological Society, 1990. All Rights Reserved

and Meixner (2001) which also used the same Horst and Weil model as the starting point of their derivation. The description of these approaches follow below.

As alluded to in Chap. 1, two important limitations of earlier solutions such as Calder's (1952), used by Gash's (1986) general solution to the diffusion equation and later applied by Schuepp et al. (1990) to quantify the flux footprint function include the constant $u/u_*$ and the limitation that these solutions are mostly applicable in neutral stability. The studies in this section represent the many efforts by the footprint community to include a height-dependent and stability-dependent wind and diffusivity profiles.

#### 3.1.3.1 The Horst and Weil (1992, 1994) Approach

Most earlier exact or approximate solutions were hampered by either or both the limitation of a constant height-independent wind speed profile and restricted to neutral stability. Following van Ulden (1978) and Horst (1979), the arrival of the Horst and Weil (1992, 1994) analytical solutions describing footprint functions provided a welcome alternative. Oversimplifications that had previously crippled solutions to the diffusion equations, i.e. that of a constant $u/u_*$ and the limitation to neutral stability, were circumvented later by Horst and Weil (1992) using a numerical solution. Horst and Weil (1994) extends their model's use to special cases of non-passive scalar transfer and became an approximate analytical solution to the diffusion equation.

Horst and Weil (1992) used the approximate vertical concentration profile equation proposed by van Ulden (1978) and Horst (1979) to formulate the crosswind-integrated flux footprint $\overline{f}^{y}(x, z_m)$ as briefly described below.

Imagining a fluid element released at a point ($x_r$, $y_r$, $z_r$) detected at a downwind position ($x$, $y$, $z$) with $Q_0(x_r, y_r, 0)$ source strength per unit area at ground-level at position ($x_r$, $y_r$, 0), the flux density measured at measurement height $z_m$ at point ($x$, $y$, $z_m$), $F(x, y, z_m)$ is given by:

$$F(x, y, z_m) = \int_{-\infty}^{\infty} \int_{0}^{\infty} Q_0(x_r, y_r, 0)f(x', y', z_m)dx_r dy_r \tag{3.6}$$

where $f(x' = x - x_r, y' = y - y_r, z_m)$ is the ***source probability density (footprint) function*** and where it is assumed that the flow field of turbulence is horizontally homogeneous. Assuming that the wind is in the x-direction (from higher to lower values), the flux footprint $f$ therefore depends only on the streamwise direction separation distance $x - x_r$ and the crosswind separation distance $y - y_r$. The sum (discrete case) or the integral (continuous) of the flux footprint values $f$ is unity.

Horst and Weil (1994, 1995) gave the special case of a surface point of emission rate $Q$ where $F_0(x_r, y_r) = Q\delta(x_r)\delta(y_r)$ with the result that the flux footprint equals the vertical flux downwind of a unit surface point source:

$$f(x, y, z_m) = \frac{F_m(x, y, z_m)}{Q} \tag{3.7}$$

Defining $\overline{f}^{y}(x, z_m)$ as the crosswind-integrated footprint, follows

$$\overline{f}^{y}(x, y, z_m) = \int_{-\infty}^{\infty} f(x, y, z_m)dy \tag{3.8}$$

and integrating the two-dimensional advection-diffusion equation from the surface to the flux measurement height $z_m$:

$$\overline{\eta_y}(x, z_m) = -\frac{\partial}{\partial x}\int_{0}^{z_m} \overline{u(z)\chi_y(x, z)}dz \tag{3.9}$$

where $\overline{u(z)}$ is the mean wind speed profile and $\overline{\chi_y(x, z)}$ is the crosswind-integrated concentration distribution downwind of a unit surface point source. Thus, the relationship between upwind surface source or sink distributions and measurements of concentration or flux at some point $z_m$ above the surface is defined by the footprint function.

Horst and Weil (1992) presented a normalized integrated crosswind integrated footprint, $\eta$, which strongly depends on $\overline{z}/z_m$ and exhibits only very weak remaining dependence on stability and surface roughness. For averaging the mean height, please see van Ulden (1978) or Eq. (2.82).

Horst and Weil (1992) demonstrated this universality by a comparison with a Lagrangian simulation footprint model. To circumvent the challenge that their model can only be evaluated numerically, Horst and Weil (1994) provided an approximate analytical expression for the normalized crosswind-integrated footprint $\Phi$ (for $A$ and $b = B^{-1}$ see Sect. 2.3.1), which is the exact solution of Eq. (3.8) for power law wind profiles (Horst 1999),

$$\Phi = \frac{z_m \overline{f}^y(x, z_m)}{d\overline{z}/dx} \approx A\left[\frac{z_m}{\overline{z}}\right]^2 \frac{\overline{u(z_m)}}{u(\overline{z})} exp^{-(z_m/b\overline{z})^r}. \tag{3.10}$$

In a tracer flux experiment aimed at validating the various footprint models available at that time, Finn et al. (1996) evaluated the parameter r experimentally for a range of atmospheric stabilities at four diffusion distances over a total of 136 cases spanning a total of 485 hypothetical towers, free of edge effects and with quality data; they did so by running their analytical model for each tracer flux period at each of the four tower distances and allowed shape parameter $r$ to vary over the range of 0.3–5.0, encompassing the theoretical limit of the Gryning et al. (1987) model. The empirical value of $r$ was then chosen as that value for which the predicted flux $F$ was equal to the measured flux.

The Horst and Weil (1992) solution has been widely used worldwide and provided invaluable insight in the analysis of field campaigns with fluxes measured over a wide variety of environmental conditions.

#### 3.1.3.2 The Schmid (1994, 1997) Approaches

A notable step forward was provided by the use of the flux footprint analytical solution originally attributed Horst and Weil (1992, 1994), see Eq. (3.10), with the arrival of the extension of the Horst and Weil formulation by Schmid (1994) to a two-dimensional flux footprint analysis, thus generating much additional insight into the interpretation of experimental data collected over patchy surfaces. Furthermore, the expanded model extended the solutions to a range of atmospheric stabilities. A useful two-dimensional source area of level $P$ defined as the integral of *hitherto* the source weight function of the smallest possible domain comprising the fraction $P$ of the total surface influence in the measured signal and based on Horst and Weil (1992) was described in Schmid (1994). The latter presented simple expressions to provide parameterization formulae for the principal source areas as functions of the measurement level, atmospheric stability, and crosswind turbulence. These formulae have ease of use but are limited in their range of applications. That model provides $P$ information.

On this basis, the original model of Schmid and Oke (1990), SAM, was extended to the two-dimensional case and not only used for the concentration footprint but also as a flux footprint model FSAM by Schmid (1994).

A later paper by Schmid (1997) discussed criteria and guidelines to be used in field campaigns over a variety of surfaces (short crops, agricultural areas, and urban areas) with particular emphasis given to the need of matching the choice of the measurement system to the spatial scale of measured surface. Schmid (1997) cautions the limits of the model regarding the range of atmospheric stability, vertical range of the applicability of the model being limited to the atmospheric surface layer, and states that flux footprints obtained from concentration profile or from Bowen ratio measurements should refer to the model of Horst (1999). For more details see Sect. 7.1.2.

The Schmid (1994) model has been one of the most useful footprint models to date owing to its inherent relevance to deal with interpretation of real-terrain sources and sinks. As is the case for all other analytical solutions, this flux footprint calculation algorithm can be tagged to signal processing packages for online analysis of flux outputs.

Unfortunately, the model is numerical unstable for $z_m/z_0 < 12$ and in highly unstable and in stable conditions. Therefore, for field applications where a wide range of atmospheric conditions is sought, the Kormann and Meixner (2001) model should be applied.

#### 3.1.3.3 The Kaharabata et al. (1997) Approach

The model by Kaharabata et al. (1997), based on the previous works by Horst and Weil (1992, 1994) and Schmid (1994), is like the later model (Kaharabata et al. 1999) a 2D approach. According to van Ulden (1978), they us the logarithmical wind profile Eq. (2.8), but multiplied the aerodynamical height in the logarithm and in the universal function with the Euler-Mascheroni constant of 0.5772. The model was mainly applied for aircraft measurements during the BOREAS experiment by Chen et al. (1999) and Ogunjemiyo et al. (2003) and further on for the emission of VOCs from forest canopies (Kaharabata et al. 1999).

#### 3.1.3.4 The Haenel and Grünhage (1999) approach

Haenel and Grünhage (1999) presented a slightly different analytical solution, which, unlike existing analytical solutions for crosswind-integrated flux footprint, normalizes the footprint using a closed analytical formula based on height-dependent profiles of wind speed and eddy diffusivity. They pointed out that the implementation of the expression above causes $\Phi$, the normalized crosswind integrated footprint, to overshoot its theoretical constraint of unity at large diffusion distances $\bar{z}(x)$.

The major difference between the Haenel and Grünhage's (1999) description and the earlier analytical flux footprint models is that the parameter $r$ shaping the vertical plume dispersion is set constant as opposed to being a function of upwind distance. As a result of this change, their model satisfies the condition that the cumulative normalized footprint approaches unity for an infinite upwind distance.

The authors proposed to keep the use of power laws expressions longer in the use of their derivation of the crosswind integration of the flux footprint expression and prescribed r as independent of $\bar{z}$ and thus of $x$. Since $r$ is a constant, the crosswind integrated flux footprint expression can be integrated numerically and becomes, in normalized form:

$$\Phi = AB'\left[\left(\frac{z_m}{b\bar{z}}\right)^{(3+r)/2}\right]\left(\frac{z_m}{b\bar{z}}\right)^{r} \tag{3.11}$$

where $B'$ is an analytical function of r in Haenel and Grünhage (1999):

$$B' = b^{(1-r)/2}\Gamma(1/r)\{\Gamma[(1+r)/2r]\}^{-1} \tag{3.12}$$

Applying Gram-Schmidt's conjugate powers for the power laws of wind speed and diffusivity, they finally reintroduced Monin-Obukhov similarity theory at this stage by expressing $r$ as a function of stability $z_m/L$ and measurement height and roughness $z_m/z_0$.

Thus, the Horst and Weil (1992, 1994) models and the Haenel and Grünhage (1999) model follow the van Ulden (1978) use of the Monin-Obukhov similarity theory for profiles of $K$ and $\bar{u}$, and ignore the weak dependence of $p$ on $r$ . The result is a similarity relation for $d\bar{z}/dx$ that can only be solved for $\bar{z}$ numerically.

The cumulative normalized footprint function approach unit asymptotically if and when the constant $m$ is defined, normally using the Gram-Schmidt's conjugate power law. This value can be defined by applying Gram-Schmidt's conjugate power law.

Haenel and Grünhage (1999) state that their model is both less complex and computationally more effective than the Horst and Weil (1994) approximate and Horst (1999) profile models.

#### 3.1.3.5 The Kormann and Meixner (2001) Approach

Both the approach of Kormann and Meixner (2001) and that of Haenel and Grünhage aim at avoiding the apparent inconsistent behavior of the Horst and Weil (1992) model and decreasing the computational time to evaluate footprint functions. Unlike Haenel and Grünhage (1999), Kormann and Meixner (2001) used the power law profiles for both $K$ and $\bar{u}$ in the solution for $d\bar{z}/dx$. It therefore allows an analytical integration.

Kormann and Meixner (2001) used two different approaches to circumvent this difficulty in solving the power-law profile, the first one resorting to the purely analytical description of Huang (1979) and a simple numerical one, which minimizes the deviations between the two different profiles. The reader is referred to Sect. 2.2.5, Eqs. (2.54)–(2.58) for details regarding the Huang (1979) method. That solution matches the power law for $u(z)$ and $K(z)$ and the Monin-Obukhov profiles for the stability dependence of the exponents in the power laws at a certain height. The numerical approach is simple when compared to that of Schmid (1994) and requires essentially a one-dimensional numerical root finding. Finally, in order to relate the two different types of profiles, we have to specify the Businger–Dyer relationships. Kormann and Meixner (2001) note further that the reference height for the exponents $p$ and $p'$ and the proportionality constants $u$ and $K$ need not be the same and that this approach generally overestimates the velocity near the ground, especially for unstable conditions and large roughness length values. In the same way, this solution tends to overestimate the eddy diffusivity in stable conditions.

In the Kormann and Meixner (2001), the original version by Huang (1979) was modified in the following form (identical with Eqs. 2.55 and 2.56)

$$p = \frac{z}{u}\frac{\partial u}{\partial z} = \frac{u_*}{\kappa u}\varphi_m(\zeta) \tag{3.13}$$

and

$$p' = \frac{z}{K}\frac{\partial K}{\partial z} = \begin{cases} \frac{1}{1+5z/L}, & L > 0 \\ \frac{1-24z/L}{1-16z/L}, & L < 0 \end{cases}. \tag{3.14}$$

In its simplest form where $p = 1$ and $p$ is the power exponent in the diffusivity expression, the Kormann and Meixner (2001) method is equivalent to that of Schuepp et al. (1990) but when Gram-Schmidt's conjugate laws must be applied ($p + p' = 1$), it is equivalent to the analytical solution of Haenel and Grünhage (1999).

To date, the Kormann and Meixner (2001) analytical solution is an algebraic expression in $x$ and $z$ and thus constitutes the only truly analytical flux footprint model based on realistic profiles of $K$ and $u$. It is one of the most desired solutions due to a combination of attributes including its ease of use, its wide range of stability and its numerical stability. An applicable version of the model was published by Neftel et al. (2008)—see also Supplement 3.1.

## Supplement 3.1: The Kormann and Meixner (2001) in the Version by Neftel et al. (2008)

The tool by Neftel et al. (2008) is available on the WEB-page:
http://www.agroscope.admin.ch/art-footprint-tool/
and includes an instruction and an EXCEL sheet. The user has to copy his input data into the EXCEL Sheet and receives as the output data for the

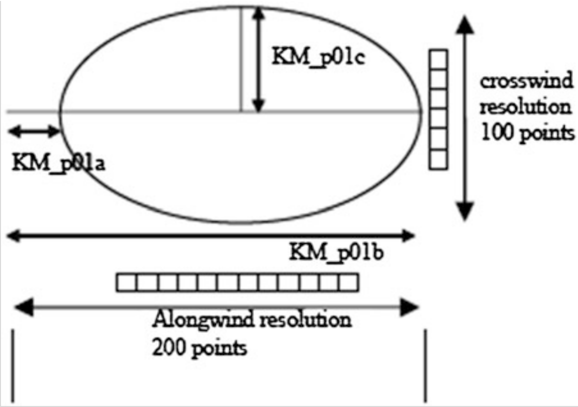


**Fig. 3.S1** Output parameter KM_p01 a, b. c of model by Neftel et al. (2008) for the 1 % effect level

footprint ellipse as given in Fig. 3.S1. The input data are given in Table 3.S1. No input of the roughness length is necessary. This is done with an internal calculation and the roughness length as an output parameter. Further output parameters are the model functions. Details are given in an instruction file.

**Table 3.S1** Input parameter of model by Neftel et al. (2008)

| | x, y Sensor coordinates | $u_*$ | L | $\sigma_v$ | Wind direction | $z_m$ | u |
|---|---|---|---|---|---|---|---|
| Dimension | m | m s$^{-1}$ | m | m s$^{-1}$ | ° | m | m s$^{-1}$ |
| Restriction | 1 m resolution | | >1 m | 0.01–5.0 m s$^{-1}$ | | Above zero plane displ. | |

## *3.1.4 Analytical Solutions Based on Lagrangian Models*

Analytical solutions have also resorted to the results and insights provided by Lagrangian simulations. Nonetheless, given that Lagrangian simulations are used to construct analytical solutions. Their linkage to analytical solutions is briefly described. Due to the release of a large number of trajectories required to obtain stable solutions, the long computing time needed to produce statistically reliable results is an unavoidable weakness of Lagrangian stochastic footprint models. This can be partly overcome using the method proposed by Hsieh et al. (2000) which sought to bypass this difficulty by using an analytical model derived from Lagrangian model results.

Hsieh et al. (2000) developed a Lagrangian stochastic dispersion model based on a Markov process and the application of the well-mixed criterion by Thomson (1987). They used the scaling and fetch analysis of previous models (Schuepp et al. 1990; Horst and Weil 1994; Luhar and Rao 1994; Hsieh et al. 1997). Finally they found that the result was very close to Gash's (1986) analytical value but describes also the flux change due to a change of the Obukhov length.

In addition, given the need for real-time footprint information during the data collection period, Kljun et al. (2004) proposed a simple parameterization based on a Lagrangian footprint model. Their parameterization is highly valuable to an experimentalist as it allows the determination of the footprint from atmospheric variables obtained during flux measurements. Kljun et al. (2004) investigated the Lagrangian backward model by Kljun et al. (2002) with an analysis of dimensionless parameters according to Buckingham's $\Pi$-Theorem (Kantha and Clayson 2000). By ensemble averaging of model runs the parameterizatious where found to be a function of following dimensionless parameters $\Pi_1 = z_m \overline{f}_y$, $\Pi_2 = x/z_m$, $\Pi_3 = z_i/z_m$, and $\Pi_4 = \sigma_w/u_*$, which could be combined finally to two parameters

$$X_* = \Pi_4^{\alpha_1} \Pi_2 = \left(\frac{\sigma_w}{u_*}\right)^{\alpha_1} \frac{x}{z_m}, \tag{3.15}$$

$$F_* = \Pi_4^{\alpha_2} \Pi_3' \Pi_1 = \left(\frac{\sigma_w}{u_*}\right)^{\alpha_2} \left(1 - \frac{z_m}{z_i}\right)^{-1} z_m \overline{f_y} \tag{3.16}$$

By ensemble averaging model runs, the parameterizations were found as functions of both dimensionless parameters (Fig. 3.2)

$$\widehat{F}_* = a \left(\frac{\widehat{X}_* + d}{c}\right)^b exp\left\{ b \left(1 - \frac{\widehat{X}_* + d}{c}\right)\right\}, \tag{3.17}$$

where $\widehat{F}_*$ and $\widehat{X_*}$ are the ensemble averaged functions, $\alpha_{1,2}$ are free parameters, and $a$, $b$, $c$, $d$ are coefficients. These parameterizations are similar to those of Hsieh et al. (2000) and are well comparable with the Kormann and Meixner (2001) analytical approach.

In comparison to the Lagrangian model the approximation is only applicable for homogeneous terrain but in comparison to many other models it can be used also outside the surface layer and was tested for a wide range of meteorological conditions: $-200 \leq z_m /L \leq 1$, $u_* \geq 0.2$ m s$^{-1}$, $z_m > 1$ m. The model is available online (Supplement 3.2).

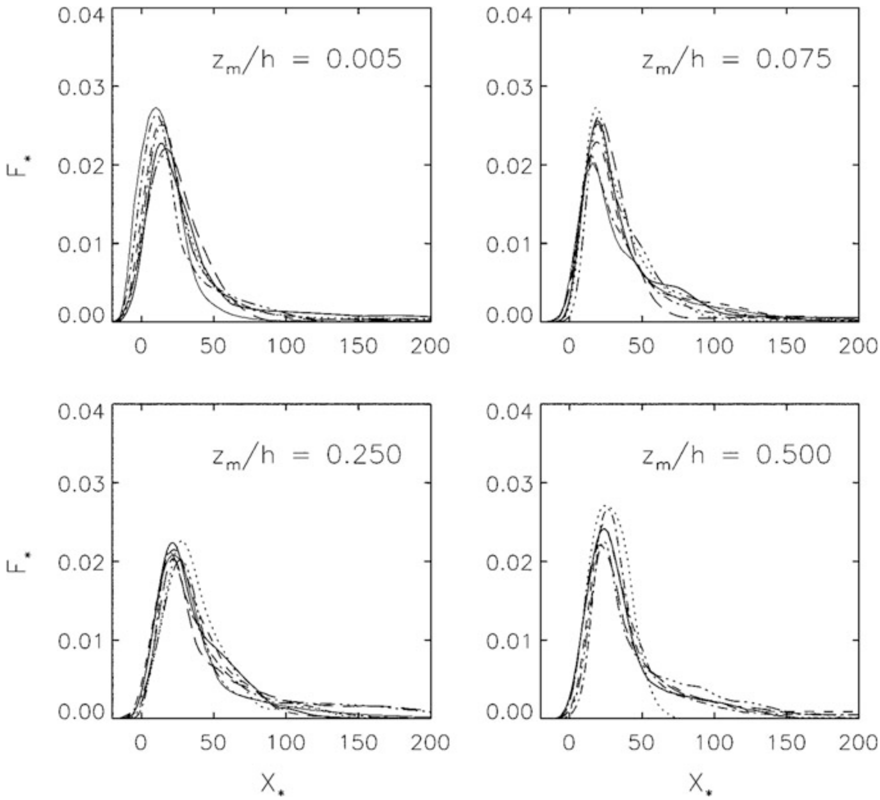


**Fig. 3.2** Parameterisation according to Kljun et al. (2004) of the ensemble of scaled flux footprints (Eq. 3.16 *solid line*). The *dashed lines* indicate the scaled footprint estimates with the backward Lagrangian model (Kljun et al. 2002). These footprint estimates range from strongly convective to strongly stable with receptor heights of $z_m/z_i = \{0.005, 0.075, 0.25, 0.50\}$. Roughness length as indicated in each panel

## Supplement 3.2: Online Version of the Model by Kljun et al. (2002) in the Analytical Version by Kljun et al. (2004)

The program by Kljun et al. (2004) is online available on the WEB-page as executable online version:
http://footprint.kljun.net/index.php
The input parameters are given in Table 3.S2. Furthermore, the effect level (up to 90 %) should be given for the calculation. The output is a visual presentation (Fig. 3.S2) and a data set of the master footprint according to in the dimensionless function

**Table 3.S2** Input parameter of model by Kljun et al. (2004)

| | $\sigma_v$ | $u_*$ | $z_m$ | $z_i$ | L | $z_0$ |
|---|---|---|---|---|---|---|
| Dimension | m $s^{-1}$ | m $s^{-1}$ | m | m | m | m |
| Restriction | | >0.2 m $s^{-1}$ | >1 m above zero plane displ. | $z_i > z_m$ | $-200 \le z_m/L \le 1$ | |

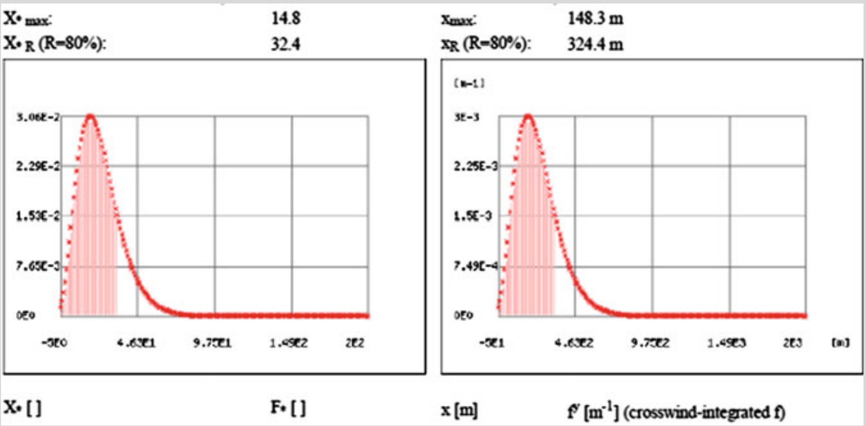


**Fig. 3.S2** Output graph of the Kljun et al. (2004) model

$$X_* = \left(\frac{\sigma_w}{u_*}\right)^{\alpha_1} \frac{x}{z_m} \tag{3.S2a}$$

and

$$F_* = \left(\frac{\sigma_w}{u_*}\right)^{\alpha_2} \left(1 - \frac{z_m}{h}\right)^{-1} z_m \overline{f^y}, \tag{3.S2b}$$

with $\alpha_1 = -\alpha_2 = 0.8$, as well as the usual crosswind integrated footprint function dependent on the distance from the measuring point. Furthermore the location of the maximum of the footprint and the extension of the footprint for the given effect level are calculated.

## 3.2 Lagrangian Simulations

The stochastic Lagrangian approach represents one of the most natural methods for simulating the motions of molecules advected in a turbulent flow to a point measurement; its approach is simple and lends itself particularly well in numerous

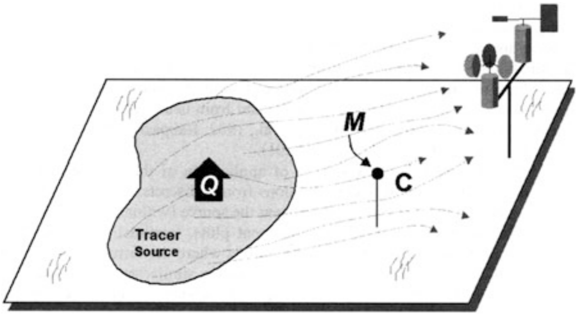


**Fig. 3.3** The inverse-dispersion method for estimating tracer emission rates (*Q*). Average tracer concentration C measured at pint M. A dispersion model predicts the ratio of concentration at M to the emission rate (*C*/*Q*) (Flesch and Wilson 2005, Published with kind permission of © American Society of Agronomy, 2005. All Rights Reserved)

footprint applications in flows ranging from homogeneous turbulence to sheared, anisotropic inhomogeneous turbulent flows. Once the form of the parameterization is chosen, the stochastic Langevin type equation is solved (e.g. Sawford 1985; Thomson 1987; Sabelfeld and Kurbanmuradov 1990). The Lagrangian approach needs only the one-point probability density function (pdf) of the Eulerian velocity field. The Lagrangian stochastic trajectory simulation, together with appropriate simulation methods and corresponding estimators for concentration or flux footprints, are then merged into a Lagrangian footprint model. For a detailed overview of the estimation of concentration and flux footprints in particular, the reader is referred to Kurbanmuradov et al. (2001).

The Lagrangian simulation (LS) method used for footprint applications involving a myriad of other atmospheric turbulent diffusion problems is based on a stochastic differential equation. That equation, the Langevin equation, determines the evolution of fluid particles in space and time. With the LS, the approach typically consists of releasing millions of fluid particles of infinitesimal mass at the surface point source and tracking their trajectories in a fluid to which a turbulent flow field is assigned and downwind of this source towards the measurement location forward in time (Fig. 3.3, Leclerc and Thurtell 1990; Rannik et al. 2000, 2003). An ensemble of particle trajectories then reproduces the dispersion process. This has the advantage that the small time behavior, i.e. the diffusion of particles for short travel times following their release, can be accounted for, something not otherwise possible in an Eulerian frame of reference (Sawford 1985; Nguyen et al. 1997). Such footprint models require a prescribed turbulence field, often obtained using scaling laws such as Monin-Obukhov similarity theory or atmospheric boundary layer scaling laws. The approach is stochastic in nature and is often treated as a Gaussian process. The idea has its origin in the “drunkard’s walk”, first coined by Einstein (1905) to describe the behavior of molecular diffusion. This reflects well the behavior of an infinitesimally small fluid particle embedded

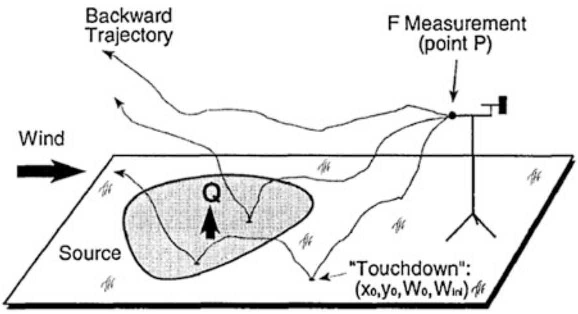


**Fig. 3.4** Idealization of the backward Lagrangian simulation methodology: Particles are released from flux measurement location (Point P) and followed upstream. A touchdown catalogue stores touchdown locations ($x_0$,$y_0$), vertical touchdown velocities ($W_0$) and vertical velocities at release ($W_{ini}$) for all particles (Flesch 1996)

in a fluid in motion. In this frame of reference and in contrast with its Eulerian counterpart, the fluid particle moves with the flow.

Lagrangian footprint models have also been run in the backward mode (Fig. 3.4), i.e. tracking the trajectories from their point of measurements back, using a negative time step, to their point of origin on the surface; this has been done for both flux and concentration footprints (Flesch and Wilson 1992; Flesch et al. 1995, 2004; Flesch 1996; Kljun et al. 2002; Cai and Leclerc 2007).

The treatment of upper and lower boundaries must be treated carefully and reflection scheme near the lower boundary developed. The literature is replete with different formulations of Lagrangian simulations for inhomogeneous turbulence, a thorny topic with theoreticians. Reviews of the myriad of formulations have been given to us by Rodean (1996), Wilson and Sawford (1996) and Kurbanmuradov and Sabelfeld (2000). Given the formulation of necessary conditions to obtain a correct simulation of diffusion in inhomogeneous turbulence, the main criterion for robust simulations is the well-mixed condition and so is correct within the most rigorous Lagrangian formulation *ab extensio*, of Lagrangian footprint models Thomson (1987). It also should be pointed out that this well-mixed criterion condition can be fulfilled. Yet, the stochastic model is not necessarily uniquely defined for atmospheric flow conditions (called the uniqueness problem). Rannik et al. (2012) point out that, even in the case of homogeneous but anisotropic turbulence, there are several stochastic models which satisfy the well-mixed condition (Thomson 1987; Sabelfeld and Kurbanmuradov 1998). In addition to the well-mixed condition by Thomson (1987), the trajectory curvature has also been proposed as the additional criterion to select the most appropriate Lagrangian stochastic model (Wilson and Flesch 1997), but this additional criterion does not define the unique model (Sawford 1999).

While many if not most Lagrangian footprint models run in the forward mode, the backward Lagrangian method has been gaining in popularity. In this scheme, particle trajectories are tracked from their point of measurements backward, using a negative timestep, to their point of origin on the surface. This has been done for both flux and concentration footprints (Flesch et al. 1995; Flesch 1996; Kljun et al. 2002; Flesch and Wilson 2005; Cai and Leclerc 2007; Hsieh and Katul 2009; Sogachev and Leclerc 2011). The basic equations for concentration and flux footprints are (Flesch 1996)

$$\chi(x, y, z) = \frac{2}{N} \sum_{i=1}^{N} \sum_{j=1}^{n_i} \frac{1}{W_{ij}} Q\left(x_{ij}, y_{ij}, z_0\right), \tag{3.18}$$

$$F(x, y, z) = \frac{2}{N} \sum_{i=1}^{N} \sum_{j=1}^{n_i} \frac{W_{i0}}{W_{ij}} Q\left(x_{ij}, y_{ij}, z_0\right), \tag{3.19}$$

with the initial velocity $W_{i0}$ and the touchdown velocity $W_{ij}$ for all particles.

The forward and backward methods used to derive footprints are theoretically equivalent. In practice, the forward LS models are generally applicable in horizontally homogeneous conditions. The attribute intrinsic in the (Flesch et al. 1995) backward trajectory approach that neither horizontal homogeneity nor stationarity of the turbulence field is required makes it in principle a powerful method to construct footprint estimates over non-homogeneous terrain. The reader is referred to Sogachev and Leclerc (2011) as an illustration.

The Lagrangian stochastic approach can be applied to any turbulence regime, thus allowing footprint calculations for various atmospheric boundary layer flow regimes. For example, in the convective boundary layer, turbulence statistics are typically non-Gaussian and for realistic dispersion simulations, a non-Gaussian trajectory model has to be applied. An indication of the departure from Gaussianity is often obtained using the turbulence velocity skewness; for instance, in convective boundary-layers, the vertical velocity skewness is typically 0.3 while a neutral canopy layer can exhibit negative vertical velocity skewness as large as −2.0 (Leclerc and Thurtell 1990; Finnigan 2000). However, most Lagrangian trajectory models fulfill the main criterion for construction of Lagrangian stochastic models, the well-mixed condition (Thomson 1987) for only one given turbulence regime.

In the case of tall forest canopies, similarity laws that work well within the atmospheric surface layer break down within the canopy, i.e. in a region characterized by fluxes rapidly changing within the canopy layer even over short distances and so the assumption of a 'constant' flux layer cannot be assumed. A theoretical framework, such as the Monin-Obukhov similarity theory, which describes time-averaged wind relations as a function of measurement height $z_m$ above the surface and atmospheric stability $z_m/L$ at any given level as long as it is contained within the atmospheric surface layer, adds a layer of complexity in the assessment of the contribution of individual source signatures to a point flux measurement, whether located within or above a canopy layer. With both thermal and mechanical turbulence most often co-arising inside a canopy layer, a sound framework to predict turbulence statistics used to identify the local footprint in

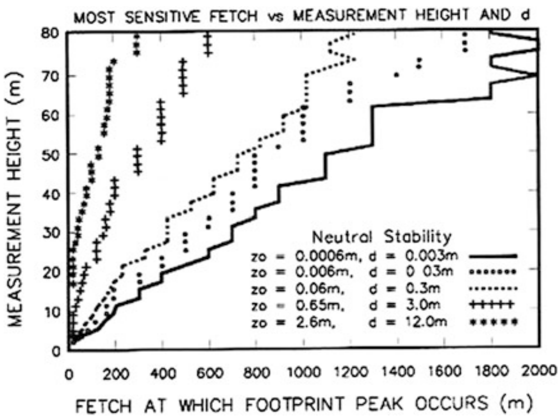


**Fig. 3.5** Dependence of the footprint peak dependent on the fetch and the measuring height (Leclerc and Thurtell 1990)

non-isothermal conditions is still needed, though recent work to palliate this deficiency is gradually emerging (Zhang et al. 2010). Also of paramount importance, knowledge of Lagrangian timescales inside a canopy is also required and, despite their capital importance in Lagrangian simulations, is still needed. Some of the Lagrangian simulations (Rannik et al. 2000; Mölder et al. 2004; Poggi and Katul 2008) also use a Kolmogorov constant $C_0$ whose model results are sensitive to the absolute value of the constant (Rannik et al. 2003; Mölder et al. 2004). Poggi and Katul (2008) revealed that $C_0$ may vary nonlinearly inside the canopy while the LS model predictions were not sensitive to gradients of $C_0$ inside canopy.

Göckede et al. (2004) solved this problem of long computing time needed to produce statistically reliable results by pre-calculation of look-up tables in a wide range of atmospheric and surface characteristics. These simplifications allow the determination of the footprint from atmospheric variables usually measured during flux observation programs.

### *3.2.1 The Leclerc and Thurtell (1990) Approach*

As one of the first two-paper series describing the behavior of flux footprint above natural surfaces, Leclerc and Thurtell (1990) investigated the signatures of individual sources contributing to a point flux measurement using a 2-D Lagrangian stochastic dispersion model parameterized by effective roughness length and displacement height (Fig. 3.5). Leclerc and Thurtell (1990) describe a two-dimensional Markovian (random walk) simulation of the respective contribution of upwind sources to a point flux measurement at height $z_m$.

This early study was the first to highlight the prominent influence of atmospheric stability on the upwind footprint; it also demonstrated the role of measurement level and surface roughness with particular attention to the location of the peak source contribution. While such results are now well accepted, their early simulations demonstrated how measurements obtained during unstable daytime conditions represent fluxes from upwind sources closer to the observation point than those measurements made during stable nighttime conditions. They also demonstrated the sensitivity of the footprint peak to measurement level and surface properties. Despite the fact that this is the first Lagrangian footprint model, its robustness was tested by several extensive turbulence tracer flux experiments and proved to be describing accurately the flux footprint over surfaces ranging from smooth surfaces to above forest canopies (Finn et al. 1996; Leclerc et al. 2003a, b)

### *3.2.2 The Sabelfeld-Rannik Approach*

The formalism of the Lagrangian simulation used by Rannik et al. (2000) to model footprints in the canopy layer is based on the work of Kurbanmuradov et al. (1999). The Kurbanmuradov-based simulation satisfies the well-mixed condition (Thomson 1987; Sabelfeld and Kurbanmuradov 1998). The Sabelfeld and Kurbanmuradov (1998) approach was compared with that of Thomson (1987) and will be shown below.

Rannik et al. (2000) evaluated both approaches, the one given by Thomson (1987) and that of Kurbanmuradov et al. (1999). A comparison between the stochastic footprint flux model using the formalism of Thomson (1987) and that of Kurbanmuradov et al. (1999) is shown in Fig. 5.1 with flux footprints found to be virtually identical to one another. Finally, the basis of this model stems from Sabelfeld and Kurbanmuradov (1990), which includes the well-mixed conditions by Thomson (1987). For the wind profile they applied the Monin-Obukhov similarity theory with a modification for the roughness sublayer according to Cellier and Brunet (1992) and an in-canopy profile according to Kaimal and Finnigan (1994). The model was tested at the FLUXNET site Vielsam (BE-Vie).

Rannik et al. (2003) improved their model by applying it to FLUXNET site Hyytiälä (FI-Hyy) data, for which they made a site specific parameterization for the in-canopy profile (see Eq. 2.68). Göckede et al. (2007) used this model for the Waldstein-Weidenbrunnen site (DE-Bay) data and found in comparison with the approach by Massman and Weil (1999) that the footprint can be significantly improved by using site specific in-canopy profile parameterizations. A further improvement is possible according to Göckede et al. (2007), if the in-canopy parameterization can be used in a specific form dependent on the coupling between the forest and the atmosphere (Thomas and Foken 2007).

### 3.2.3 The Kljun et al. (2002) 3D Backward Lagrangian Footprint Model

The study of Kjun et al. (2002) is credited for the first use a 3D backward Lagrangian footprint model (LPDM-B) to determine flux footprints using the three-dimensional model of de Haan and Rotach (1998). The latter, based on Rotach et al. (1996) uses the approach of backward Lagrangian dispersion method first attributed to Flesch et al. (1995). The Kljun et al. (2002) model accommodates a wide spectrum of atmospheric stabilities and satisfies the well-mixed condition throughout a wide range of stabilities. It also can be used in three-dimensional footprint calculations above the surface layer, something particularly useful in the interpretation of observations from airborne flux platforms (Leclerc et al. 1997). Following Rotach et al. (1996), Kljun et al. (2002) approximated a skewed probability density function of the vertical velocity to model the footprint in the convective boundary layer using a scheme proposed by Baerentsen and Berkowicz (1984) in their LPDM-B. This approximation was done by adding the sum of two Gaussian distributions one for the updrafts and one for the downdrafts respectively. Gibson and Sailor (2012) found some mathematical inconsistencies in the Rotach et al. (1996) and therefore also in the Kljun et al. (2002) approach. The correction would make the model more stable.

Based on Flesch's method (personal comm., 2001), Kljun et al. (2002) also introduced a spin-up procedure in the model. The simulated flux footprint depends strongly on the particle's initial velocities since these are explicitly included in the footprint calculation. According to the authors, Lagrangian particle models need to incorporate the correlation of the streamwise and vertical velocity components resulting in unrealistic individual particle velocities produced. Assuming this to be the case, when calculated over hundreds of thousands of particles, this effect is non-negligible and biases the trajectories, and thus the resulting concentrations. While the distributions without spin-up were almost symmetric (neglected correlation of $u$ and $w$) in the quadrant analysis (not shown here), the spin-up procedure leads to a more realistic distribution between the flow quadrants. The figures below depict the footprint flux and concentration results of the LPDM-B for contrasting stability conditions (Figs. 3.6 and 3.7).

Also based on the approach by Flesch et al. (1995) Wang and Rotach (2010) developed a backward model for undulating surfaces in a non-flat topography. They found that the topographic influence on the footprint depends on the stratification, the wind speed and the wind direction in relative to the orientation of the topography.

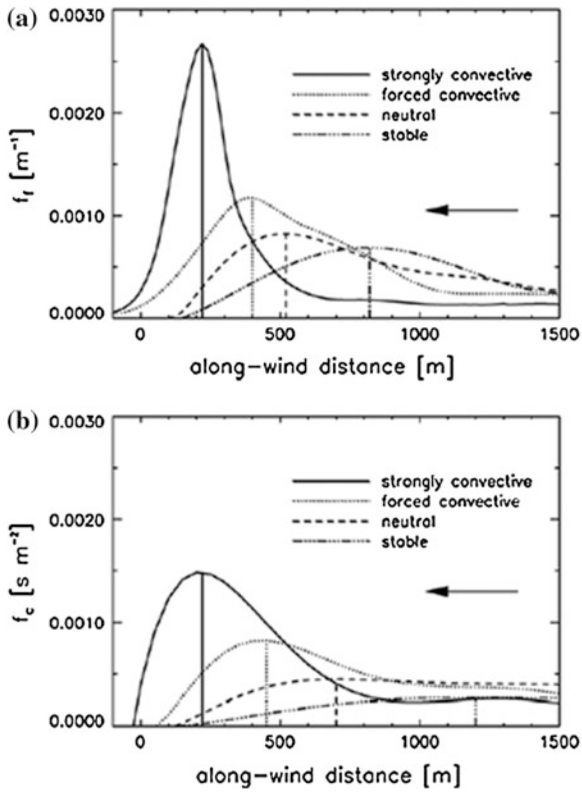


**Fig. 3.6** **a** Crosswind integrated footprint for flux and **b** concentration measurements for four different cases of stability. The location of respective peaks are indicated by *vertical lines* (Kljun et al. 2002)

## 3.3 Higher-Order Closure Footprint Models

An alternative to analytical solutions or to Lagrangian formalism arises in the form of higher-order closure models. These can be used to describe a step change in contrasting scalar flux in two adjoining fields with dissimilar scalar and aerodynamic properties provided the change from an upwind mixing length to a downwind equilibrium value is gradual. Amongst these, the second-order closure model is the closure order most often sought.

One recent member of this family of higher-order closure models, SCADIS, uses one and half order closure scheme: this two-equation model bypasses a predefined mixing length and includes a new parameterization for the drag term (Sogachev and Lloyd 2004). The numerical atmospheric boundary-layer (ABL) SCADIS model based on $E$-$\omega$ scheme (where $E$ is turbulent kinetic energy and $\omega$ is specific dissipation of $E$) is a model that has been rapidly gaining ground because of its versatility as described in Sogachev et al. (2002, 2005a), Sogachev and Lloyd (2004) and in Sogachev and Leclerc (2011).

Model equations and details for SCADIS numerical schemes and boundary conditions and further improvements to the parameterization can be found in

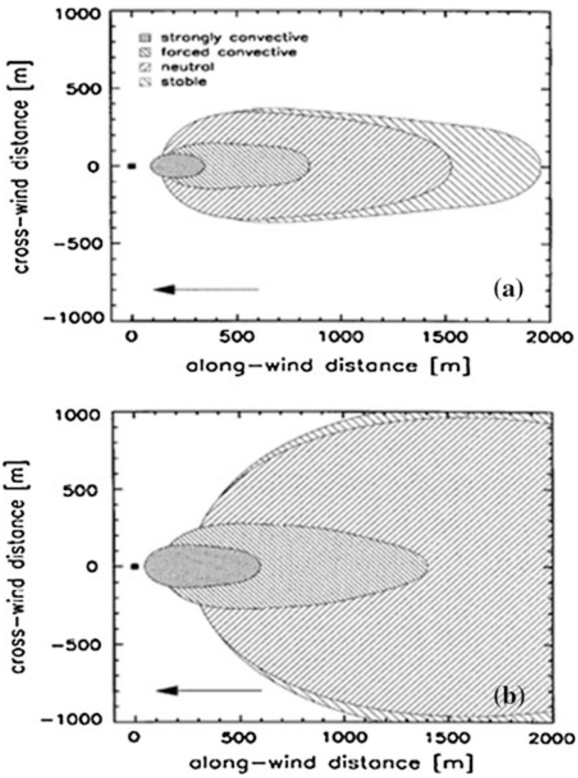


**Fig. 3.7** **a** 50 % source area flux and **b** concentration measurements for four different cases of stability. The *square* indicates the receptor location (Kljun et al. 2002)

Sogachev and Lloyd (2004) and Sogachev et al. (2002, 2005a, b, 2008). In SCADIS, the two-dimensional governing equations solved are those for mass and momentum conservation (Navier-Stokes). To date, SCADIS has been used in footprint quantification over short crops, tall forest canopies, urban canopies, in downwind of clearcuts in a forest canopy. It has also recently been coupled to a Lagrangian Particle Dispersion Model (LPDM) ran in an inverse mode to determine the concentration footprint from tall towers (Sogachev and Leclerc 2011).

## 3.4 Large-Eddy Simulation Models

The advantage of LES compared to conventional footprint models lies in its ability to determine turbulence statistics, scalar fluxes and concentrations and thus to evaluate the corresponding footprints without the use of externally-derived turbulence statistics. Numerous workers have used this method to further their insight into footprints and apply it to a range of surface and flow properties (Leclerc et al. 1997; Cai and Leclerc 2007; Prabha et al. 2008; Steinfeld et al. 2008). Figure 3.8 presents the comparison of Langrangian and LES simulation for the concentration

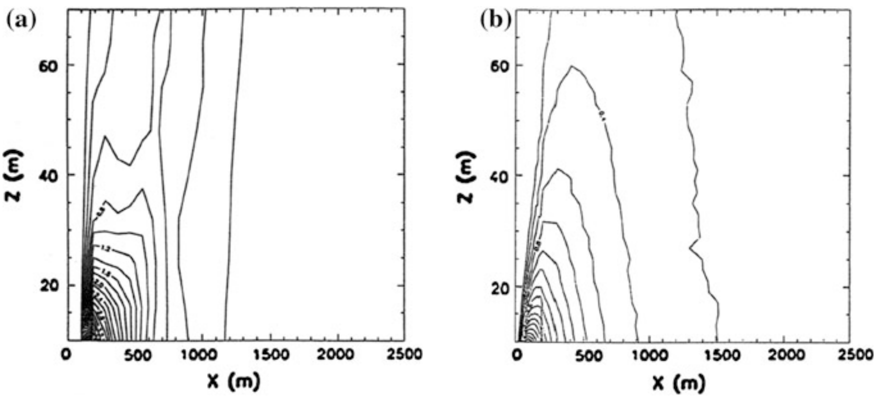


**Fig. 3.8** Contours of the normalized crosswind integrated concentration in the surface layer as a function of the downwind distance *x*. **a** Large eddy simulation and **b** Lagrangian stochastic model (Leclerc and Thurtell 1990), L = −32 m in both models (Leclerc et al. 1997, Published with kind permission of © American Geophysical Union (Wiley), 2012. All Rights Reserved)

field according to Leclerc et al. (1997). Furthermore, the LES method has been applied to simulate footprints in the convective boundary layer (Leclerc et al. 1997; Guo and Cai 2005; Cai and Leclerc 2007; Peng et al. 2008; Prabha et al. 2008; Steinfeld et al. 2008).

In recent studies (Cai and Leclerc 2007; Steinfeld et al. 2008) the LES simulation was used in conjunction with the Lagrangian simulation at the sub-grid scale to model convective boundary layer turbulence and infer concentration footprints (Cai and Leclerc 2007; Cai et al. 2008, 2010); Steinfeld et al. (2008) used LES to describe the footprint in boundary layers of different complexities. The Steinfeld et al. (2008) study compared their results with the Finn et al. (1996) tracer flux footprint study and the LES flux footprint of Leclerc et al. (1997). More details can be found in Sect. 3.5.

## 3.5 Hybrid Footprint Models

A new breed of models which we will call ‘hybrid’ models is becoming increasingly popular owing to the increased computational speed. There is a rapidly growing proliferation of models seeking to harness the sophistication and advantages of different models, most often combining Eulerian and Lagrangian-generated statistics to solve practical problems in difficult atmospheric flows.

## 3.5.1 LES-Driven Lagrangian Stochastic Models

### 3.5.1.1 The Prabha et al. (2008) Approach

Examples include the work of Prabha et al. (2008) who first used the turbulence statistics obtained using the LES to drive a Lagrangian stochastic footprint model with a coupling in an offline mode. This strategy can be advantageous when LES is used as a standard technique for turbulence simulation allowing an evaluation of the performance of the Lagrangian simulation of footprints inside canopies. This point is interesting specially when considering that there is a paucity of tracer experiments in-canopy combining turbulence measurements with tracer information.

The Prabha et al. (2008) study solves the conservation equations for mass and momentum and TKE in a three-dimensional domain following Shaw and Patton (2003). The Lagrangian footprint model follows the Thomson criteria (1987) with algorithms for the coefficients of the Fokker-Planck equation based on Flesch and Wilson (1992) accounting for inhomogeneous anisotropic turbulence. Prabha et al. (2008) use on offline coupling of the two models whereby the LES data are saved at a certain timestep and from there, the data are used to run the LES.

They then used the LES-derived turbulent flow statistics as an input to a stochastic footprint model of Flesch and Wilson (1992). That study used several different Lagrangian timescale formulations in the Lagrangian simulations and compared their sensitivity to the resulting flux footprints and compared the results against those obtained with the LES simulations.

### 3.5.1.2 The Cai and Leclerc (2007) and Cai et al. (2008) Approach

Hybrid models have also been used successfully by Cai and Leclerc (2007) to drive a Lagrangian stochastic model with LES data. The authors used a turbulence field derived from the LES of a passive tracer to drive both forward and backward models in an effort to derive convective boundary layer concentration footprints. They derived concentration footprints at four levels in the convective boundary layer using both forward and backward models. They also used the two models in the reverse direction, i.e. using the stochastic simulation to parameterize sub-grid scale turbulence in the LES. Cai and Leclerc (2007) noted that there is equivalence between the results in horizontally homogeneous turbulence and that while the forward method agreed with laboratory experimental results (Willis and Deardorff 1976, 1978, 1981) for different release heights in the convective boundary layer results from backward dispersion are asymmetric in contrast with the forward method. The authors point out that the backward dispersion results show crosswind-integrated concentration footprints in a generalized sense, i.e. where concentration from all sources, ground and elevated, are included, not just those at the

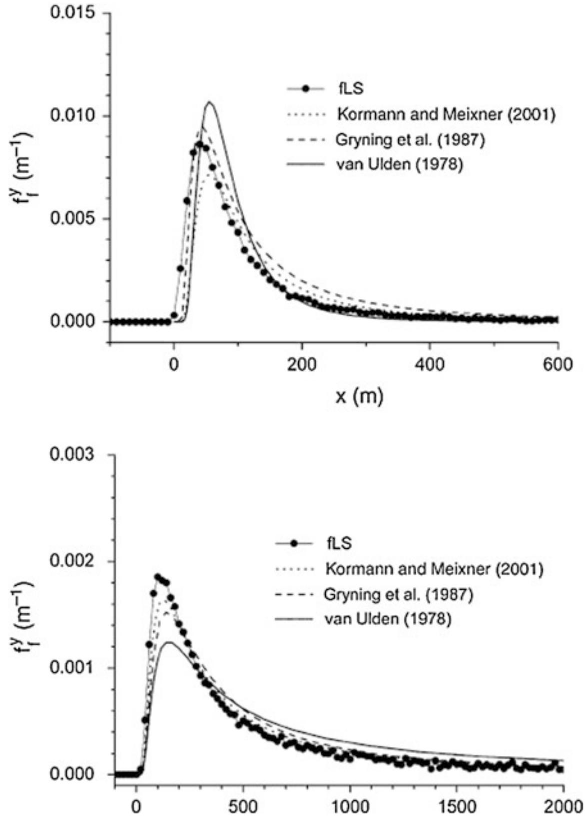


**Fig. 3.9** Crosswind-integrated flux footprints of three analytical models and that of the forward LS model. Two stability cases with Obukhov length $L$ equals (*above*) –16 m (*below*) 40 m. The *horizontal* coordinate denotes upwind distances (Cai et al. 2008)

surface. Furthermore Cai et al. (2008) show that the proposed model is in a good agreement with analytical models for concentration and flux footprints (Fig. 3.9).

### *3.5.2 LES-Embedded Lagrangian Stochastic Models: The Steinfeld et al. (2008) Approach*

Steinfeld et al. (2008) also used a combination of LES coupled to a Lagrangian dispersion model to calculate footprints in both homogeneously- and heterogeneously-driven boundary layers. In their case, it is the Large-Eddy Simulation which is driven by the output of the Lagrangian model (Fig. 3.10). They documented positive and negative flux footprints in the convective boundary layer, as had been reported previously by Prabha et al. (2008) inside a forest canopy.

Results from these two studies are consistent with those of Finnigan's (2004) conclusion that the flux footprint function is a function of the concentration footprint function and in complex flows there is no guarantee that the flux footprint is positive, bounded by zero and one.

What really sets the Steinfeld et al. (2008) approach apart from the other LS-LES coupled models is (i) that the coupling of the two is done online and (ii) that the Lagrangian simulation of trajectories is embedded as a set of sub-routines in the LES code. The authors use that approach to evaluate the footprints obtain over a heterogeneously-heated convective boundary layer. The Steinfeld et al. (2008) LES code follows that of Raasch and Etling (1998) and Raasch and Schröter (2001) while the version of the Lagrangian model follows the method proposed by Thomson (1987).

## *3.5.3 Higher-Order Closure-Driven Lagrangian Simulation*

The first such study was done by Luhar and Rao (1994), followed by Kurbanmuradov et al. (2003), and recently by Hsieh and Katul (2009) who applied a stochastic model to estimate footprint and water vapor fluxes over inhomogeneous surfaces. The latter derived the turbulence field of the two-dimensional flow over a change in surface roughness using a combination of both closure model and performed Lagrangian simulations to evaluate the footprint functions.

### 3.5.3.1 The Luhar and Rao (1994) Approach

The work presented by Luhar and Rao (1994) is also a coupled footprint model. They used a one dimensional second-order closure model of Rao et al. (1974) for the atmospheric boundary layer to account for the effects of vegetation on surface energy and water balance through a 'big-leaf' approach to determine the footprint for latent heat fluxes measured at various locations and heights near the surface. That model has a timescale determined by the model itself, not specified a priori, since the model includes a dynamical equation for the energy dissipation. These flow fields thus obtained were then used to drive the Lagrangian simulation to calculate footprints for cases where the flow is transitioning from an arid region to an irrigated crop field, changing the partitioning of net radiation into sensible and latent heat fluxes (Fig. 3.11).

### 3.5.3.2 The Hsieh and Katul (2009) Approach

While Hsieh and Katul (2009) resort to the use of stand-alone Lagrangian simulation to model the footprint over homogeneous surfaces. They used a Lagrangian simulation driven by a second-order closure scheme to determine the footprint flux

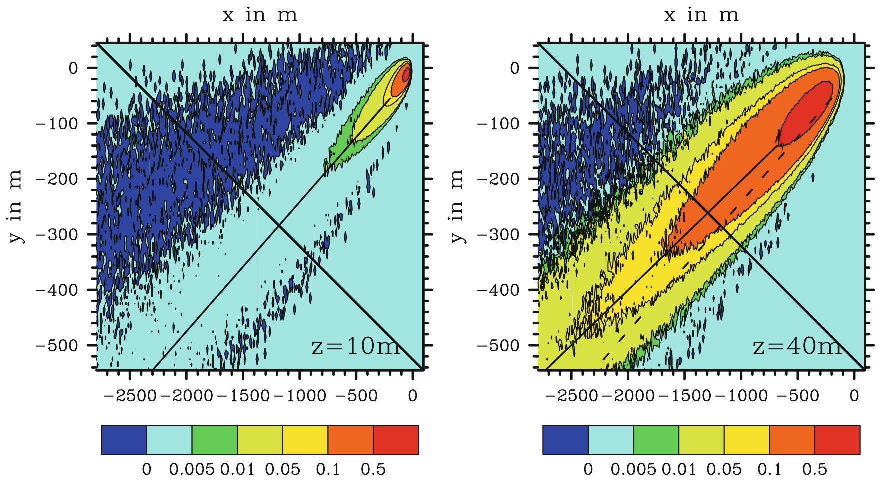


**Fig. 3.10** Flux footprints normalized by the respective maximum value evaluated for the period between 7 and 9 a.m. local time after the start of the simulation for measurement heights of 10 and 40 m in the conventional neutral boundary layer (Steinfeld et al. 2008)

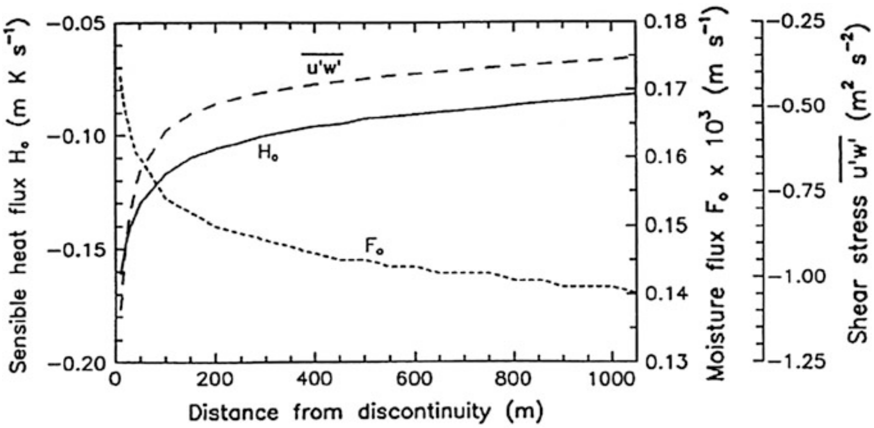


**Fig. 3.11** Variation of surface fluxes of momentum ($u'w'$), sensible heat ($H_0$) at latent heat ($E_0$) flux over a wet grassy surface (Luhar and Rao 1994)

over inhomogeneous terrain involving a step change in surface source. Their Lagrangian model incorporates the fluctuating component of the streamwise velocity component and is two-dimensional, a feature that few Lagrangian stochastic footprint models incorporate. The Lagrangian simulation is particularly useful in planar inhomogeneous terrain. Given that the step change in temperature and moisture conditions over the domain precludes the use of Monin-Obukhov similarity theory to generate the fields of temperature and moisture, a second-order model was used. The closure formulations used are those of Wichmann and

Schaller (1986). Chap. 4 discusses results of comparisons of water vapor fluxes obtained from experimental data that shows agreement with the output of this Eulerian-Lagrangian coupled model.

#### 3.5.3.3 E-ω Model Closure-Driven Lagrangrian Simulation

A recent approach is being used to broaden and extend the scope of footprint modeling in the atmospheric boundary layer. Seeking to obtain the concentration footprint to determine the spatial extent of the location of sources upwind from concentration measurements in the upper boundary layer using a tall-tower, Sogachev and Leclerc (2011) used a $E$-$\omega$ model (1.5 order closure model) called SCADIS, and embedded it into a Lagrangian simulation. They then examined concentration footprints from nocturnal tall tower measurements with and without the presence of a low-level jet (Sogachev and Leclerc 2011). The hybridization for these models is done in an offline mode. The model was run in the forward mode to examine the evolution of the spread of marked fluid particles and in the backward mode to determine the concentration footprint.

SCADIS incorporates meteorological variables which are dependent on net radiation and incoming solar radiation, surface roughness, sky conditions and initial air temperature profiles. The full description of SCADIS can be found in Sogachev et al. (2002, 2008). In their paper, Sogachev and Leclerc (2011) used SCADIS to drive a Lagrangian model in backward mode to determine the concentration footprints from a tall tower at a 500 m level.

The Lagrangian simulation used by the authors is based on the work of Legg and Raupach (1982) and in backward mode. The Lagrangian simulation used by Sogachev and Leclerc (2011) uses a spin up procedure as per Kljun et al. (2002). The coupled model is then used to create concentration footprints, over a series of terrain conditions, eddy diffusivity and atmospheric stability throughout a 12-h period.

## References

Baerentsen JH, Berkowitz R (1984) Monte Carlo simulation of plume dispersion in the convective boundary layer. Atmos Environm 18:701–712

Cai X, Peng G, Guo X, Leclerc MJ (2008) Evaluation of backward and forward Lagrangian footprint models in the surface layer. Theor Appl Climat 93:207–233

Cai X, Leclerc MY (2007) Forward-in-time and backward-in-time dispersion in the convective boundary layer: the concentration footprint. Boundary-Layer Meteorol 123:201–218

Cai X, Chen J, Desjardins R (2010) Flux Footprints in the convective boundary layer: large-eddy simulation and lagrangian stochastic modelling. Boundary-Layer Meteorol 137:31–47

Calder KL (1952) Some recent British work on the problem of diffusion in the lower atmosphere. In: Proceedings of the US technology conference on air pollution. McGraw Hill, New York, pp 787–792

Cellier P, Brunet Y (1992) Flux-gradient relationships above tall plant canopies. Agric Forest Meteorol 58:93–117

Chen JM, Leblanc SG, Cihlar J, Desjardins RL, MacPherson IJ (1999) Extending aircraft- and tower-based $CO_2$ flux measurements to a boreal region using a Landsat thematic mapper land cover map. J Geophys Res 104(D14):16859–816877

de Haan P, Rotach MW (1998) A novel approach to atmospheric dispersion modelling: the Puff-Particle Model (PPM). Q J Roy Meteorol Soc 124:2771–2792

Einstein A (1905) Über die von der molekularkinetischen Theorie der Wärme geforderte Bewegung von in ruhenden Flüssigkeiten suspendierten Teilchen. Ann Phys 17:549–560

Finn D, Lamb B, Leclerc MY, Horst TW (1996) Experimental evaluation of analytical and Lagrangian surface-layer flux footprint models. Boundary-Layer Meteorol 80:283–308

Finnigan J (2000) Turbulence in plant canopies. Ann Rev Fluid Mech 32:519–571

Finnigan J (2004) The footprint concept in complex terrain. Agric Forest Meteorol 127:117–129

Flesch TK, Wilson JD (1992) A two-dimensional trajectory-simulation model for non-Gaussian inhomogeneous turbulence within plant canopies. Boundary-Layer Meteorol 61:349–374

Flesch TK, Wilson JD, Yee E (1995) Backward-time Lagrangian stochastic dispersion models and their application to estimate gaseous emissions. J Appl Meteorol 34:1320–1332

Flesch TK (1996) The footprint for flux measurements, from backward Lagrangian stochastic models. Boundary-Layer Meteorol 78:399–404

Flesch TK, Wilson JD, Harper LA, Crenna BP, Sharpe RR (2004) Deducing ground-air emissions from observed trace gas concentrations: a field trial. J Appl Meteorol 43:487–502

Flesch TK, Wilson JD (2005) Estimating tracer emissions with backward Lagrangian stochastic technique. In: Hatfield JL, Baker JM (eds) Micrometeorology in agricultural systems. American Society of Agronomy, Madison, pp 513–531

Gash JHC (1986) A note on estimating the effect of a limited fetch on micrometeorological evaporation measurements. Boundary-Layer Meteorol 35:409–414

Gibson M, Sailor D (2012) Corrections to the mathematical formulation of a backwards Lagrangian particle dispersion model. Bound-Layer Meteorol 145:399-406

Göckede M, Rebmann C, Foken T (2004) A combination of quality assessment tools for eddy covariance measurements with footprint modelling for the characterisation of complex sites. Agric Forest Meteorol 127:175–188

Göckede M, Thomas C, Markkanen T, Mauder M, Ruppert J, Foken T (2007) Sensitivity of Lagrangian stochastic footprints to turbulence statistics. Tellus 59B:577–586

Gryning SE, Holtslag AAM, Irvin JS, Sivertsen B (1987) Applied dispersion modelling based on meteorological scaling parameters. Atmos Environ 21:79–89

Guo XF, Cai XH (2005) Footprint characteristics of scalar concentration in the convective boundary layer. Adv Atmos Sci 22:821–830

Haenel H-D, Grünhage L (1999) Footprint analysis: a closed analytical solution based on height-dependent profiles of wind speed and eddy viscosity. Boundary-Layer Meteorol 93:395–409

Horst TW (1979) Lagrangian similarity modeling of vertical diffusion from a ground level source. J Appl Meteorol 18:733–740

Horst TW, Slinn WGN (1984) Estimates for pollution profiles above finite area-sources. Atmos Environm 18:1339–1346

Horst TW, Weil JC (1992) Footprint estimation for scalar flux measurements in the atmospheric surface layer. Boundary-Layer Meteorol 59:279–296

Horst TW, Weil JC (1994) How far is far enough?: the fetch requirements for micrometeorological measurement of surface fluxes. J Atmos Ocean Technol 11:1018–1025

Horst TW, Weil JC (1995) Corrigenda: how far is far enough?: the fetch requirements for micrometeorological measurement of surface fluxes. J Atmos Ocean Technol 12:447

Horst TW (1999) The footprint for estimation of atmosphere-surface exchange fluxes by profile techniques. Boundary-Layer Meteorol 90:171–188

Hsieh C-I, Katul GG, Schieldge J, Sigmon JT, Knoerr KK (1997) The Lagrangian stochastic model for fetch and latent heat flux estimation above uniform and non-uniform terrain. Water Resour Res 33:427–428

Hsieh C-I, Katul G, Chi T-W (2000) An approximate analytical model for footprint estimation of scalar fluxes in thermally stratified atmospheric flows. Adv Water Res 23:765–772

Hsieh C-I, Katul G (2009) The Lagrangian stochastic model for estimating footprint and water vapor fluxes over inhomogeneous surfaces. Int J Biometeorol 53:87–100

Huang CH (1979) A theory of dispersion in turbulent shear flow. Atmos Environ 13:453–463

Kaharabata SK, Schuepp PH, Ogunjemiyo S, Shen S, Leclerc MY, Desjardins RL, MacPherson JI (1997) Footprint considerations in BOREAS. J Geophys Res 102(D24):29113–29124

Kaharabata SK, Schuepp PH, Fuentes JD (1999) Source footprint considerations in the determination of volatile organic compound fluxes from forest canopies. J Appl Meteorol 38:878–884

Kaimal JC, Finnigan JJ (1994) Atmospheric boundary layer flows: their structure and measurement. Oxford University Press, New York 289 pp

Kantha LH, Clayson CA (2000) Small scale processes in geophysical fluid flows. Academic Press, San Diego 883 pp

Kljun N, Rotach MW, Schmid HP (2002) A three-dimensional backward Lagrangian footprint model for a wide range of boundary layer stratification. Boundary-Layer Meteorol 103:205–226

Kljun N, Calanca P, Rotach M, Schmid HP (2004) A simple parameterization for flux footprint predictions. Boundary-Layer Meteorol 112:503–523

Kormann R, Meixner FX (2001) An analytical footprint model for non-neutral stratification. Boundary-Layer Meteorol 99:207–224

Kurbanmuradov O, Rannik U, Sabelfeld KK, Vesala T (1999) Direct and adjoint Monte Carlo for the footprint problem. Monte-Carlo Meth Appl 5:85–111

Kurbanmuradov O, Sabelfeld KK (2000) Lagrangian stochastic models for turbulent dispersion in atmospheric boundary layers. Boundary-Layer Meteorol 97:191–218

Kurbanmuradov O, Rannik Ü, Sabelfeld KK, Vesala T (2001) Evaluation of mean concentration and fluxes in turbulent flows by Lagrangian stochastic models. Math Comput Simul 54:459–476

Kurbanmuradov O, Levykin A, Rannik Ü, Sabelfeld K, Vesala T (2003) Stochastic Langrarian footprint calculations over a surface with an abrupt change of roughness height. Monte-Carlo Methods Appl 9:167–188

Leclerc MY, Thurtell GW (1990) Footprint prediction of scalar fluxes using a Markovian analysis. Boundary-Layer Meteorol 52:247–258

Leclerc MY, Shen S, Lamb B (1997) Observations and large-eddy simulation modeling of footprints in the lower convective boundary layer. J Geophys Res 102(D8):9323–9334

Leclerc MY, Karipot A, Prabha T, Allwine G, Lamb B, Gholz HL (2003a) Impact of non-local advection on flux footprints over a tall forest canopy: a tracer flux experiment (Special issue: Advances in micrometeorology: Tribute to G. W. Thurtell). Agric Forest Meteorol 115:19–30

Leclerc MY, Meskhidze N, Finn D (2003b) Comparison between measured tracer fluxes and footprint modeling predictions over a homogeneous canopy of intermediate roughness. Agric Forest Meteorol 117:145–158

Legg BJ, Raupach MR (1982) Markov-chain simulation of particle dispersion in inhomogeneous flows: the mean drift velocity induced by a gradient in Eulerian velocity variance. Boundary-Layer Meteorol 24:3–13

Luhar AK, Rao KS (1994) Source footprint analysis for scalar fluxes measured in flows over an inhomogeneous surface. In: Gryning SE, Millan MM (eds) Air pollution modeling and its applications. Plenum Press, New York, pp 315–323

Massman WJ, Weil JC (1999) An analytical one-dimensional second-order closure model of turbulence statistics and the Lagrangian time scale within and above plant canopies of arbitrary structure. Boundary-Layer Meteorol 91:81–107

Mölder M, Klemedtsson L, Lindroth A (2004) Turbulence characteristics and dispersion in a forest—verification of Thomson's random-flight model. Agric Forest Meteorol 127:203–222

Neftel A, Spirig C, Ammann C (2008) Application and test of a simple tool for operational footprint evaluations. Environ Pollut 152:644–652

Nguyen AT, Budker D, DeMille D, Zolotorev M (1997) Search for parity nonconservation in atomic dysprosium. Phys Rev A56:3453–3463

Ogunjemiyo SO, Kaharabata SK, Schuepp PH, MacPherson IJ, Desjardins RL, Roberts DA (2003) Methods of estimating $CO_2$, latent heat and sensible heat fluxes from estimates of land cover fractions in the flux footprint. Agric Forest Meteorol 117:125–144

Pasquill F (1972) Some aspects of boundary layer description. Q J Roy Meteorol Soc 98:469–494

Peng G, Cai X, Zhang H, Li A, Hu F, Leclerc MY (2008) Heat flux apportionment to heterogeneous surfaces using flux footprint analysis. Adv Atm Sci 25:107–116

Poggi D, Katul GG (2008) Turbulent intensities and velocity spectra for bare and forested gentle hills: flume experiments. Boundary-Layer Meteorol 129:25–46

Prabha T, Leclerc MY, Baldocchi D (2008) Comparison of in-canopy flux footprints between Large-Eddy Simulation and the Langrangian simulation. J Appl Meteorol Climatol 47:2115–2128

Raasch S, Etling D (1998) Modeling deep ocean convection: large eddy simulation in comparison with laboratory experiments. J Phys Ocean 28:1796–1802

Raasch S, Schröter M (2001) PALM—a large-eddy simulation model performing on massively parallel computers. Meteorol Z 10:363–372

Rannik Ü, Aubinet M, Kurbanmuradov O, Sabelfeld KK, Markkanen T, Vesala T (2000) Footprint analysis for measurements over heterogeneous forest. Boundary-Layer Meteorol 97:137–166

Rannik Ü, Markkanen T, Raittila T, Hari P, Vesala T (2003) Turbulence statistics inside and above forest: influence on footprint prediction. Boundary-Layer Meteorol 109:163–189

Rannik Ü, Sogachev A, Foken T, Göckede M, Kljun N, Leclerc MY, Vesala T (2012) Footprint analysis. In: Aubinet M et al (eds) Eddy covariance: a practical guide to measurement and data analysis. Springer, Berlin, pp 211–261

Rao KS, Wyngaard JC, Coté OR (1974) The structure of the two-dimensional internal boundary layer over a sudden change of surface roughness. J Atmos Sci 31:738–746

Rodean HC (1996) Stochastic Lagrangian models of turbulent diffusion. Am Meteorol Soc, Boston 84 pp

Rotach MW, Gryning S-E, Tassone C (1996) A two-dimensional Lagrangian stochastic dispersion model for daytime conditions. Q J Roy Meteorol Soc 122:367–389

Sabelfeld KK, Kurbanmuradov OA (1990) Numerical statistical model of classical incompressible isotropic turbulence. Sov J Numer Anal Math Model 5:251–263

Sabelfeld KK, Kurbanmuradov OA (1998) One-particle stochastic Lagrangian model for turbulent for turbulent dispersion in horizontally homogeneous turbulence. Monte-Carlo Meth Appl 4:127–140

Sawford BL (1985) Lagrangian statistical simulation of concentration mean and fluctuation fields. J Appl Meteorol Climatol 24:1152–1166

Sawford BL (1999) Rotation of trajectories in Lagrangian stochastic models of turbulent dispersion. Boundary-Layer Meteorol 93:411–424

Schmid HP, Oke TR (1990) A model to estimate the source area contributing to turbulent exchange in the surface layer over patchy terrain. Q J Roy Meteorol Soc 116:965–988

Schmid HP (1994) Source areas for scalars and scalar fluxes. Boundary-Layer Meteorol 67:293–318

Schmid HP (1997) Experimental design for flux measurements: matching scales of observations and fluxes. Agric Forest Meteorol 87:179–200

Schuepp PH, Leclerc MY, MacPherson JI, Desjardins RL (1990) Footprint prediction of scalar fluxes from analytical solutions of the diffusion equation. Boundary-Layer Meteorol 50:355–373

Shaw RH, Patton EG (2003) Canopy element influences on resolved- and subgrid-scale energy within a large-eddy simulation. Agric Forest Meteorol 115:5–17

Sogachev A, Menzhulin G, Heimann M, Lloyd J (2002) A simple three dimensional canopy-planetray boundary layer simulation model for scalar concentrations and fluxes. Tellus 54B:784–819

Sogachev A, Lloyd J (2004) Using a one-and-a-half order closure model of atmospheric boundary layer for surface flux footprint estimation. Boundary-Layer Meteorol 112:467–502

Sogachev A, Leclerc MJ, Karipot A, Zhang G, Vesala T (2005a) Effect of clearcuts on footprints and flux measurements above a forest canopy. Agric Forest Meteorol 133:182–196

Sogachev A, Panferov O, Gravenhorst G, Vesala T (2005b) Numerical analysis of flux footprints for different landscapes. Theor Appl Clim 80:169–185

Sogachev A, Leclerc MY, Zhang G, Rannik U, Vesala T (2008) $CO_2$ fluxes near a forest edge: a numerical study. Ecol Appl 18:1454–1469

Sogachev A, Leclerc MY (2011) On concentration footprints for a tall tower in the presence of a nocturnal low-level jet. Agric Forest Meteorol 151:755–764

Steinfeld G, Raasch S, Markkanen T (2008) Footprints in homogeneously and heterogeneously driven boundary layers derived from a Langrangian stochastic particle model embedded into large-eddy simulation. Boundary-Layer Meteorol 129:225–248

Thomas C, Foken T (2007) Flux contribution of coherent structures and its implications for the exchange of energy and matter in a tall spruce canopy. Boundary-Layer Meteorol 123:317–337

Thomson DJ (1987) Criteria for the selection of stochastic models of particle trajectories in turbulent flows. J Fluid Mech 189:529–556

van Ulden AP (1978) Simple estimates for vertical diffusion from sources near the ground. Atmos Environ 12:2125–2129

Wang W, Rotach M (2010) Flux footprints over an undulating surface. Boundary-Layer Meteorol 136:325–340

Wichmann M, Schaller E (1986) On the determination of the closure parameters in high-order closure models. Boundary-Layer Meteorol 37:323–341

Willis GE, Deardorff JW (1976) A laboratory model of diffusion into the convective planetary boundary. Q J Roy Meteorol Soc 102:427–445

Willis GE, Deardorff JW (1978) A laboratory model of dispersion from an elevated source within a modeled convective planetary boundary. Atmos Environ 12:1305–1312

Willis GE, Deardorff JW (1981) A laboratory model of dispersion from a source in the middle of the convectively mixed layer. Atmos Environ 15:109–117

Wilson JD, Sawford BL (1996) Review of Lagrangian stochastic models for trajectories in the turbulent atmosphere. Boundary-Layer Meteorol 78:191–210

Wilson JD, Flesch TK (1997) Wind and remnant tree sway in forest openings III. A wind flow model to diagnose spatial variation. Agric Forest Meteorol 93:259–282

Zhang G, Leclerc MY, Karipot A (2010) Local flux-profile relationships of wind speed and temperature in a canopy layer in atmospheric stable conditions. Biogeosciences 7:3625–3636